Research Square

Preprints are preliminary reports that have not undergone peer review.
They should not be considered conclusive, used to inform clinical practice,
or referenced by the media as validated information.

Enhanced PRL-1 expression in placenta-derived mesenchymal stem cells accelerates hepatic function via mitochondrial dynamics in a cirrhotic rat model

Jae Yeon Kim
CHA University
Jong Ho Choi
Gangneung-Wonju National University
Ji Hye Jun
CHA University
Sohae Park
CHA University
Jieun Jung
CHA University
Si Hyun Bae
Catholic University of Korea School of Medicine
Gi Jin Kim (gjkim@cha.ac.kr)
CHA University https://orcid.org/0000-0002-2320-7157

Research

Keywords: Chronic liver fibrosis, Mitochondria, Phosphatase of regenerating liver-1, Placenta-derived mesenchymal stem cells

Posted Date: April 15th, 2020

DOI: https://doi.org/10.21203/rs.3.rs-22313/v1

License: This work is licensed under a Creative Commons Attribution 4.0 International License.
Read Full License

Version of Record: A version of this preprint was published on November 27th, 2020. See the published version at https://doi.org/10.1186/s13287-020-02029-3.

Abstract

Background: Placenta-derived mesenchymal stem cells (PD-MSCs) have been highlighted as an alternative cell therapy agent that becomes a next-generation stem cell treatment because of several advantages, including therapeutic effects in regenerative medicine and potential as vehicles for targeted gene delivery systems. Phosphatase of regenerating liver-1 (PRL-1), an immediate early gene, plays a critical role during liver regeneration. However, whether enhanced PRL-1 expression in cirrhotic liver accelerates the mitochondrial metabolic state for hepatic regeneration remains unknown. Here, we generated enhanced PRL-1 in PD-MSCs (PD-MSCsPRL-1, PRL-1+) using lentiviral and nonviral gene delivery systems and investigated mitochondrial functions by PD-MSCPRL-1 transplantation for hepatic functions in a rat model with bile duct ligation (BDL).

Methods: PD-MSCsPRL-1 were generated by lentiviral and non-viral AMAXA gene delivery systems and analyzed for their characteristics and mitochondrial metabolic functions. Sprague-Dawley (SD) rats induced liver cirrhosis using common BDL for 10 days. PKH67+ naïve and PD-MSCsPRL-1 using a non-viral system (2x106 cells/animal) were intravenously administered into cirrhotic rats. The animals were sacrificed at 1, 2, 3, and 5 weeks after transplantation and engraftment of stem cells, and histopathological analysis and hepatic mitochondrial functions were performed.

Results: PD-MSCsPRL-1 using lentiviral and non-viral AMAXA systems were successfully generated, and they maintained characteristics similar to those of naïve cells. PD-MSCsPRL-1 improved respirational metabolic states in mitochondria compared with naïve cells. In particular, compared with mitochondria in PD-MSCsPRL-1 generated by the nonviral AMAXA system, mitochondria in PD-MSCsPRL-1 generated by the lentiviral system showed a significant increase in the respirational metabolic state, including ATP production and mitochondrial biogenesis (*$p<0.05$). Furthermore, transplantation of PD-MSCsPRL-1 using a nonviral AMAXA system promoted engraftment into injured target liver tissues of a rat cirrhotic model with BDL and enhanced the metabolism of mitochondria via increased mtDNA and ATP production, thereby improving therapeutic efficacy.

Conclusions: Our findings will further our understanding of the therapeutic mechanism of enhanced MSCs and provide useful data for the development of next-generation MSC-based cell therapy and therapeutic strategies for regenerative medicine in liver disease.

Background

Regenerative medicine using stem cells is a new promising field for treating damaged organs and various degenerative diseases, such as difficult to treat hepatic failure disease. Various stem cells have the capacity to ameliorate liver damage in animal models of hepatic failure. Chronic liver disease is characterized by permanent changes to the liver and is associated with poor outcomes and high mortality. Although the most effective therapy for acute hepatic failure and advanced cirrhosis is liver

transplantation, this procedure has several limitations, including surgical complications, immunological suppression and high medical cost [1].

The alternative function of mitochondria in the liver following hepatic failure is important for liver regeneration [2]. Hepatic diseases cause defects in mitochondrial structure and function as the mitochondria in the hepatocytes of patients with nonalcoholic steatohepatitis are swollen and exhibit abnormal morphology with a loss of cristae; additionally, in these patients, the activities of mitochondrial respiratory complexes are impaired, and mitochondrial oxidative stress is increased [3, 4]. Moreover, the dynamics of mitochondrial biogenesis are essential to liver regeneration [5]. Augmenter of liver regeneration knockdown inhibits mitochondrial transcription factor A (mtTFA) and peroxisome proliferator-activated receptor-gamma coactivator-1 alpha (PGC-1α), resulting in impaired mitochondrial biogenesis [6].

In hepatic failure diseases, hepatic restoration by bone marrow-derived mesenchymal stem cell (BM-MSC) transplantation is associated with the mitochondria-dependent pathway [7]. The therapeutic action of MSCs in liver disease was postulated to include differentiation into hepatocytes or fusion with endogenous hepatocytes [8]. In addition to this multidifferentiative potential, MSCs reduce liver injury by ameliorating oxidative stress through the release of antioxidants and antifibrotic effects [9]. MSCs with increased Bcl-2 expression improve the recovery of liver function in carbon tetrachloride (CCl_4)-induced hepatic cirrhotic rats [10]. Recently, autologous MSC transplantation into patients with hepatic diseases was attempted in clinical trials [11, 12]. Clinical trials have shown that BM-MSC transfusion can improve hepatic function [13]. In a phase 2 trial with seventy-two patients, autologous BM-MSCs were associated with reductions in the proportion of collagen and improvement in measures of liver function [14]. Although hepatic function tests were improved in several patients, the trial triggered side effects [15]. In particular, isolation of autologous MSCs in patients has limitations, including pain and a lack of fresh MSCs harvested from patients.

Placenta-derived mesenchymal stem cells (PD-MSCs) have very strong immune-modulatory privileges [16]. PD-MSCs can modulate the immune functions of macrophages and dendritic cells, leading to inhibition of T cell proliferation or promotion of the generation of regulatory T cells [17]. Recently, we reported that increased autophagy induced by PD-MSC transplantation promotes hepatic regeneration in a CCl_4-injured rat liver model [18]. In addition, epigenetic alterations induced by PD-MSCs through the interleukin-6 (IL-6)/signal transducer and activator of transcription 3 (STAT3) signaling pathway improve liver regeneration [19]. MicroRNA-125b from PD-MSCs suppressed the activation of the Hedgehog signaling pathway, suggesting that it reduced hepatic fibrosis [20]. Moreover, human placental MSC administration significantly decreased transforming growth factor- β1 and alpha smooth muscle actin expression and enhanced liver function in CCl_4-induced fibrotic rats [21].

Phosphatase of regenerating liver-1 (PRL-1), a protein tyrosine phosphatase, was originally identified as an immediate early gene in liver regeneration [22]. Mitogenic upregulation of PRL-1 and increased portal flow by early growth response factor-1 (Egr-1) activation is an early event in liver regeneration [23]. The

function of PRL-1 is to promote cell migration and invasion by stimulating matrix metalloproteinase (MMP)-2 and − 9 expression via the Src kinase and ERK1/2 pathways; additionally, PRL-1 binds to p115 Rho GTPase-activating protein [24, 25]. Ectopic expression of PRL-1 increases Rho levels, which have a critical role in actin filament assembly and stabilization of focal adherin [26]. PRL-1 expression protects cells from apoptosis and is essential for normal timing of cell cycle progression during liver regeneration [27]. Moreover, PRL-1 regulates hematopoietic stem cell behavior [28, 29].

However, the effect of enhanced PRL-1 expression in PD-MSCs (PD-MSCs^{PRL-1}, PRL-1+) on mitochondrial function properties in hepatic cirrhotic liver remains unclear. Therefore, the objective of this study is to generate stable PD-MSCs^{PRL-1} using lentiviral and non-viral systems and compare their characteristics and demonstrate their therapeutic effects on liver function through the mitochondrial metabolic pathway in a rat cirrhosis model established by bile duct ligation (BDL).

Materials And Methods

Cell culture

Placentas at term (≥ 37 gestational weeks) were assembled from women without medical, obstetrical, and surgical complications. The collection of samples and their use for research purposes were approved by the IRB of CHA General Hospital, Seoul, Korea (IRB 07–18). All participating women provided written, informed consent. PD-MSCs were harvested as previously described [30]. PD-MSCs were maintained in alpha-modified minimal essential medium (α-MEM; HyClone, Logan, UT, USA) supplemented with 10% fetal bovine serum (FBS; Gibco, Carlsbad, CA, USA), 1% penicillin/streptomycin (P/S; Gibco), 25 ng/ml human fibroblast growth factor-4 (hFGF-4) (PeproTech, Rocky Hill, NJ, USA), and 1 μg/ml heparin (Sigma-Aldrich, St. Louis, MO, USA). Isolated primary hepatocytes from seven-week-old male Sprague-Dawley (SD) rats (Orient Bio Inc., Seongnam, Korea) using a two-step collagenase perfusion process were cultured in William's E medium (Sigma-Aldrich) supplemented with 10% FBS (Gibco), 1% P/S (Gibco), and 4 mM L-glutamine (Gibco). To induce cholestatic injury in primary hepatocytes, 100 μM lithocholic acid (LCA) was applied for 12 h. Naïve and PD-MSCs^{PRL-1} (1×10^5 cells) were seeded onto Transwell inserts (8-μm pore size; Corning, NY, USA). Cells were maintained at 37 ℃ in a humidified atmosphere containing 5% CO_2.

Gene transfections

PRL-1 plasmid (human protein tyrosine phosphatase type 4 A, member 1; PTP4A1) was purchased (Origene Inc., Rockville, MD, USA) and used to induce the overexpression of the PRL-1 gene. CMV6-AC vector containing PRL-1, the GFP reporter gene, CMV promoters and the antibiotic neomycin was digested with Sgf1 and Mlu1 restriction enzymes. PRL-1 lentiviral plasmid was purchased (SeouLin Bioscience, Seongnam, Korea). pLenti-RSV-EF1α vector including PRL-1 was constructed with a C-terminal GFP as well as the antibiotic puromycin. AMAXA pCMV-GFP vector was contained (Lonza, Basel, Switzerland). The resulting plasmid was confirmed by DNA sequencing. Naïve PD-MSCs (6×10^4 cells/cm^2) were

harvested and transfected by using an AMAXA system with a Human MSC Nucleofector Kit (Lonza) and lentiviral vector (SeouLin Bioscience). After transfections by each system, cells generated using AMAXA were selected by 1.5 mg/ml neomycin. In addition, cells generated using lentiviral vector were selected by 2 μg/ml puromycin for 7 days. We changed the medium every other day and observed changes in cell morphology. Cells were maintained at 37 ℃ in a humidified atmosphere containing 5% CO_2.

Animal models and transplantation of MSCs

Seven-week-old male SD rats (Orient Bio Inc.) were housed under specific pathogen-free conditions. Liver cirrhosis was induced by common BDL as previously described [31]. Naïve (TTx Naïve; $n = 20$) and PD-MSCs^{PRL-1} (TTx PRL-1+; $n = 20$) (2×10^6 cells, 9–10 passages) were stained with PKH67 Fluorescent Cell Linker Kit (Sigma-Aldrich) and transplanted through the tail vein. Non-transplanted (NTx; $n = 20$) rats were maintained as well as sham controls (Con; $n = 5$). After 1, 2, 3 and 5 weeks, the rats were sacrificed, and their liver tissues and blood were harvested. Alanine aminotransferase (ALT), aspartate aminotransferase (AST), total bilirubin (TBIL), and albumin levels using separated serum from the blood were measured (Southeast Medi-Chem Institute, Busan, Korea). In all animal experimental processes, protocols were approved by the Institutional Review Board (IRB) of CHA General Hospital, Seoul, Korea (IACUC-180023).

Histopathological and immunofluorescence analysis

To confirm the induction of liver cirrhosis with BDL and engraftment into target injured tissue for histological examination, liver specimens for each group ($n = 5$) were collected and fixed in 10% neutral buffered formalin (NBF). Samples were embedded in paraffin and OCT compound and processed as 5-μm thick sections for hematoxylin & eosin (H&E), Sirius red, Masson's trichrome, and PKH67+ (green) signal. 4',6-diamidino-2-phenylindole (DAPI) (Invitrogen, Carlsbad, CA, USA) was used as a counterstain for immunofluorescence. Morphometric images of whole sections in liver were captured using a digital slide scanner (3DHISTECH Ltd., Budapest, Hungary).

Reverse transcription & quantitative real-time polymerase chain reaction (PCR) analysis

Total RNA was extracted from samples with TRIzol LS Reagent (Invitrogen). cDNA was synthesized by reverse transcription from total RNA (500 ng) using SuperScript III reverse transcriptase (Invitrogen) according to the manufacturer's instructions. To analyze stemness and hepatogenic differentiation markers of naïve and PD-MSCs^{PRL-1}, PCR amplification was performed with specific primers (Table 1, designed by BIONEER, Daejeon, Korea). β-actin was used as an internal control.

Table 1

Primer sequences using reverse transcription polymerase chain reaction

Genes		Primer sequences	Tm
Oct4	Forward	5'-AGTGAGAGGCAACCTGGAGA-3'	52
	Reverse	5'-GTGAAGTGAGGGCTCCCATA-3'	
Nanog	Forward	5'-TTCTTGACTGGGACCTTGTC-3'	52
	Reverse	5'-GCTTGCCTTGCTTTGAAGCA-3'	
Sox2	Forward	5'-GGGCAGCGTGTACTTATCCT-3'	52
	Reverse	5'-AGAACCCCAAGATGCACAAC-3'	
HLA-G	Forward	5'-GCGGCTACTACAACCAGAGC-3'	58
	Reverse	5'-GCACATGGCACGTGTATCTC-3'	
TERT	Forward	5'-GAGCTGACGTGGAAGATGAG-3'	55
	Reverse	5'-CTTCAAGTGCTGTCTGATTCCAATG-3'	
Albumin	Forward	5'-TGAGTTTGCAGAAGTTTCCA-3'	60
	Reverse	5'-CCTTTGCCTCAGCATAGTTT-3'	
β-actin	Forward	5'-TCCTTCTGCATCCTGTCAGCA-3'	58
	Reverse	5'-CAGGAGATGGCCACTGCCGCA-3'	

To assess differentiation, migration, mitochondrial biogenesis and albumin expression of samples, qRT-PCR was performed with human and rat primers (Tables 2 and 3, designed by BIONEER) and SYBR Green Master Mix (Roche, Basel, Switzerland) in a CFX Connect™ Real-Time System (Bio-rad, Hercules, CA, USA). Target gene expression was normalized to GAPDH, and the 2-ΔΔCT method generated the relative values of mRNA expression. All reactions were performed in triplicate.

Table 2

Human primer sequences using quantitative real time polymerase chain reaction

Genes		Primer sequences	Tm
OC	Forward	5'-CACTCCTCGCCCTATTGGC-3'	58
	Reverse	5'-CCCTCCTGCTTGGACACAAAG-3'	
COL1A1	Forward	5'-AGACATCCCACCAATCACCT-3'	60
	Reverse	5'-CGTCATCGCACAACACCT-3'	
Adipsin	Forward	5'-GGTCACCCAAGCAACAAAGT-3'	60
	Reverse	5'-CCTCCTGCGTTCAAGTCATC-3'	
PPAR-γ	Forward	5'-TTGACCCAGAAAGCGATTCC-3'	60
	Reverse	5'-AAAGTTGGTGGGCCAGAATG-3'	
PRL-1	Forward	5'-TACTGCTCCACCAAGAAGCC-3'	60
	Reverse	5'-AGGTTTACCCCATCCAGGTC-3'	
h-RhoA	Forward	5'-TGGAAAGCAGGTAGAGTTGG-3'	60
	Reverse	5'-GACTTCTGGGGTCCACTTTT-3'	
ROCK1	Forward	5'-GAAGAAAGAGAAGCTCGAGA-3'	60
	Reverse	5'-GATCTTGTAGCTCCCGCATCTGT-3'	
Alu	Forward	5'-GGAGGCTGAGGCAGGAGAA-3'	55
	Reverse	5'-CGGAGTCTCGCTCTGTCGCCCA-3'	
PGC-1α	Forward	5'-CAGCAAAAGCCACAAAGACG-3'	60
	Reverse	5'-GGGTCAGAGGAAGAGATAAAGTTG-3'	
NRF1	Forward	5'-GCTTCAGAATTGCCAACCAC-3'	60
	Reverse	5'-GTCATCTCACCTCCCTGTAAC-3'	
mtTFA	Forward	5'-GAACAACTACCCATATTTAAAGCTCA-3'	60
	Reverse	5'-GAATCAGGAAGTTCCCTCCA-3'	
mtDNA	Forward	5'-CCACTGTAAAGCTAACTTAGCATTAACC-3'	55
	Reverse	5'-GTGATGAGGAATAGTGTAAGGAGTATGG-3'	
nuclearDNA	Forward	5'-CCAGAAAATAAATCAGATGGTATGTAACA-3'	55
	Reverse	5'-TGGTTTAGGAGGGTTGCTTCC-3'	

Genes		Primer sequences	Tm
GAPDH	Forward	5'-GCACCGTCAAGGCTGAGAAC-3'	60
	Reverse	5'-GTGGTGAAGACGCCAGTGGA-3'	

Table 3
Rat primer sequences using quantitative real time polymerase chain reaction

Genes		Primer sequences	Tm
PGC-1α	Forward	5'-GTGCAGCCAAGACTCTGTATGG-3'	60
	Reverse	5'-GTCCAGGTCATTCACATCAAGTTC-3'	
NRF1	Forward	5'-GCTGTCCCACTCGTGTCGTAT-3'	60
	Reverse	5'-GTTTGAGTCTAACCCATCTATCCG-3'	
mtTFA	Forward	5'-CGCCTAAAGAAGAAAGCACA-3'	60
	Reverse	5'-GCCCAACTTCAGCCATTT-3'	
mtD-Loop	Forward	5'-GGTTCTTACTTCAGGGCCATCA-3'	55
	Reverse	5'-GATTAGACCCGTTACCATCGAGAT-3'	
β-actin	Forward	5'-GGGATGTTTGCTCCAACCAA-3'	55
	Reverse	5'-GCGCTTTTGACTCAAGGATTTAA-3'	
GAPDH	Forward	5'-TCCCTCAAGATTGTCAGCAA – 3'	60
	Reverse	5'-AGATCCACAACGGATACATT-3'	

Western blotting

To assess specific gene expression of PD-MSCs^{PRL-1} and cirrhotic liver tissues, samples were lysed in protein lysis buffer (Sigma-Aldrich). The protein lysates were loaded on sodium dodecyl sulfate polyacrylamide gels, and separated proteins were transferred to PVDF membrane. The following primary antibodies were used: anti-human PRL-1, anti-Oct4 (1:1,000; all from Abcam, Cambridge, UK), anti-albumin, anti-HLA-G (4h84) (1:1,000; all from Novus Biologicals, Littleton, CO, USA), anti-ATP5B (1:200; Santa Cruz Biotechnology, Dallas, TX, USA), anti-ROCK1, anti-RhoA, anti-CDK4, anti-cyclin D1, and mitochondrial marker antibody sampler kit (1:1000; all from Cell Signaling Technology, Denvers, MA, USA). The loading control was anti-GAPDH (1:3,000; AbFrontier, Seoul, Korea). The following secondary antibodies were used: anti-mouse IgG (1:5,000; Bio-Rad, Hercules, CA, USA) and anti-rabbit IgG (1:10,000; Bio-Rad). The bands were detected using ECL reagent (Bio-Rad).

Multilineage differentiation analysis

To induce adipogenic and osteogenic differentiation, PD-MSCs^{PRL-1} (5 passages) generated using lentiviral and AMAXA systems were plated (5×10^3 cells/cm^2) in each differentiation induction medium using a StemPro Adipogenesis and Osteogenesis differentiation kit (Gibco). Each medium was changed every other day. After approximately 21 days, cells were fixed with 4% paraformaldehyde and incubated for 1 h with Oil Red O (Sigma-Aldrich) for staining lipids and von Kossa with 5% silver nitrate (Sigma-Aldrich) to visualize the calcium deposits.

To induce hepatogenic differentiation, PD-MSCs^{PRL-1} (5 passages) were seeded (5×10^3 cells/cm^2) in low-glucose Dulbecco's-modified Eagle medium (DMEM; HyClone) supplemented with 40% MCDB 201 medium (Sigma-Aldrich), 2% FBS, and 1% P/S coated with 5 μg/ml type IV collagen. After 48 h, the growth medium was replaced with low-glucose DMEM supplemented with 20 ng/ml epidermal growth factor (EGF; Peprotech), 10 ng/ml basic fibroblast growth factor (bFGF; Peprotech), 10 ng/ml bone morphogenetic protein-4 (Peprotech), 40% MCDB 201 medium, and 1% P/S. Then, PD-MSCs^{PRL-1} were cultured for an additional 48 h. The cells were treated for another week in step-1 medium consisting of low-glucose DMEM supplemented with 20 ng/ml hepatocyte growth factor (Peprotech), 10 ng/ml bFGF, 40% MCDB 201 medium, 2% FBS, and 1% P/S to progress to the maturation step. Then, differentiation was induced by incubating PD-MSCs^{PRL-1} for another week with step-2 medium consisting of low-glucose DMEM supplemented with 20 ng/ml oncostatin M (Peprotech), 1 μM dexamethasone (Sigma-Aldrich), 1 × ITS + Premix (Sigma-Aldrich), 40% MCDB 201 medium, 2% FBS, and 1% P/S. During steps 1 and 2, the culture media were changed every other day. After 18 days, each plate of PD-MSCs^{PRL-1} were incubated for 1 h at 37 °C with 1 mg/ml indocyanine green (ICG) (Dong in Dang Pharm., Siheung, Korea) uptake as described previously [30].

FACS analysis

PD-MSCs^{PRL-1} (5 passages) were stained with monoclonal antibodies specific for the following proteins to phenotype cell-surface antigens: CD34 (PE), CD90 (PE), HLA-ABC (FITC), HLA-DR (FITC) (BD Bioscience, San Diego, CA, USA), CD13 (PE) (BioLegend, San Diego, CA, USA), CD105 (PE) (R&D Systems, Minneapolis, MN, USA), and HLA-G (FITC) (Abcam). After staining, cells were washed in PBS and treated with appropriate isotype antibodies (BD Biosciences, San Jose, CA, USA). Cells were analyzed by a FACSCalibur flow cytometer (Becton Dickinson, Franklin Lakes, NJ, USA). For each sample, at least 10,000 events were acquired.

Teratoma formation

To confirm teratoma formation by PD-MSCs^{PRL-1}, nine-week-old male nonobese diabetic/severe combined immunodeficiency (NOD/SCID) mice (Laboratory animal Research Center, Bungdang CHA medical center, Seongnam, Korea) were housed in an air-conditioned animal facility under pathogen-free conditions. A total of 5×10^5 cells of each cell type (lenti and AMAXA) was transplanted into one testis (Tx; $n = 2$). The other testis was not injected (Con; $n = 2$). After testes were maintained for 14 weeks, mice were sacrificed and testes of all groups were collected. Each section of testis tissue was stained with H&E.

Migration assay

Naïve and PD-MSCs^{PRL-1} (2×10^4 cells) were seeded into the upper inserts of a Transwell chamber (8-μm pore size; Corning) with or without siRNA-PRL-1 after 24 h to analyze the migration ability of naïve and PD-MSCs^{PRL-1}. Each cell type was fixed with 100% methanol for 10 min and then stained with Mayer's hematoxylin (Dako, Santa Clara, CA, USA) for 5 min. The number of stained cells was randomly counted in eight non-overlapping fields on the membranes at a magnification of 200×. The experiments were performed in triplicate.

L-lactate production assay

To confirm the end product of glycolysis in naïve and PD-MSCs^{PRL-1}, the lactate production rate was determined using a colorimetric L-lactate assay kit (Abcam). Cell lysates were deproteinized to eliminate endogenous LDH by a Deproteinizing Sample Preparation Kit–TCA (Abcam). Each sample was plated in a 96-well plate and added lactate reagent for 30 min. The absorbance was quantified using an Epoch microplate reader (BioTek, Winooski, VT, USA) at 450 nm. The lactate concentration was evaluated by the trend line equation. The experiments were conducted in triplicate.

Measurement of ATP production

To confirm that mitochondria provide energy, ATP concentrations of homogenized liver tissue samples, PD-MSCs^{PRL-1}, primary hepatocyte lysate were measured by an ATP determination kit (ThermoFisher Scientific, Waltham, MA, USA). According to the manufacturer's instructions, ATP concentrations were assessed using a microplate reader (BioTek) at 570 nm. The experiments were detected in triplicate.

Mitochondrial DNA (mtDNA) copy number assay

Genomic DNA (gDNA) was extracted from MSCs, primary hepatocytes, and homogenized BDL-injured rat liver to analyze mtDNA copy number. qRT-PCR amplification was conducted with specific primers (Table 2) containing 250 ng of gDNA, primers of nuclear DNA with FAM- and mtDNA with JOE-labeled quencher dye, 1 × Taqman Universal Master Mix (Applied Biosystems, Foster City, CA, USA) according to the manufacturer's instructions. Data were obtained in triplicate.

XF mito stress assay

To further analyze mitochondrial metabolic functions in live PD-MSCs^{PRL-1}, an XF24 Extracellular Flux Analyzer (Seahorse Bioscience, North Billerica, MA, USA) was assessed for real-time analysis of the oxygen consumption rate (OCR) and extracellular acidification rate (ECAR). Naïve and PD-MSCs^{PRL-1} were plated on XF24-well microplates (Seahorse Bioscience) (7×10^3 cells/well). The cells were adjusted for the equilibrium in XF buffer for 60 min for contemporaneous analysis of OCR and ECAR by repeated cycles of mixing (3 min), incubation (2 min) and measurement (3 min) periods in a non-CO_2 incubator. Following basal respiration measurements, the cells were sequentially treated with 0.5 μM oligomycin, 0.5 μM carbonyl cyanide-*p*-trifluoromethoxyphenylhydrazone (FCCP), 1 μM rotenone/antimycin A (AA)

mixture. The changes in respiration were recorded. The Seahorse XF24 Analyzer program was set according to the manufacturer's recommendation. OCR/ECAR was then normalized by total cell number.

Statistical analysis

All data were expressed as the mean ± standard deviation (SD). Student's *t*-test was used for analysis, and *p* values less than 0.05 were considered statistically significant. All experiments were conducted in triplicate.

Results

Generation of stable PD-MSCs with PRL-1 using lentiviral and non-viral AMAXA systems

Naïve PD-MSCs at passage 8 were transfected with lentiviral and non-viral AMAXA plasmid tagged GFP to overexpress PRL-1 in PD-MSCs (PD-MSCs^{PRL-1}, PRL-1+). A positive control was used for the GFP vector. After transfection, PD-MSCs generated using lentiviral vector containing 2 μg/ml puromycin and AMAXA containing 1.5 mg/ml neomycin were stabilized in conditioned medium (Fig. 1a). GFP-positive PD-MSCs^{PRL-1} using each system maintained spindle-like and fibroblastoid morphologies similar to those of MSCs (Fig. 1b). Also, overexpression of PRL-1 was confirmed in PD-MSCs^{PRL-1} compared to naïve (Fig. 1c). In addition, RT-PCR results in PD-MSCs^{PRL-1} revealed the expression of stemness markers (Oct4, Nanog, and Sox2) and telomerase reverse transcriptase (TERT). In particular, human leukocyte antigen (HLA)-G, which has an immunomodulatory effect, was expressed in both cell types (Fig. 1d).

We previously confirmed characterization of naïve PD-MSCs [32]. The immunophenotypes of both types of PD-MSCs^{PRL-1} were analyzed by flow cytometry. MSC markers cluster of differentiation (CD13, CD90, and CD105) were positive, whereas the hematopoietic and endothelial cell marker CD34 was negative in both types of PD-MSCs^{PRL-1}. Moreover, HLA-DR was nearly absent. However, HLA-ABC and HLA-G were significantly positive in PD-MSCs^{PRL-1} (Fig. 1e). The protein levels of both cell types were higher than those of naïve (Fig. 1f). Nine-week-old male NOD/SCID mice were directly injected with PD-MSCs^{PRL-1} into the testes (n = 2; lentiviral, n = 2; AMAXA) to confirm teratoma formation in vivo. Mice were sacrificed at 14 weeks postinjection, and each testis was evaluated by H&E staining (Fig. 1g) and the human-specific Alu sequence from gDNA isolation. Testes injected with cells treated with both systems had no teratomas, and Alu expression was higher in injected testes than in non-injected testes (Fig. 1h). These findings indicated that PRL-1 overexpressing PD-MSCs were generated using lentiviral and non-viral AMAXA systems and maintained characteristics similar to those of naïve cells.

Multidifferentiation potential of PD-MSCs^{PRL-1}

PD-MSCs^{PRL-1} that differentiated into mesodermal lineages (osteogenic and adipogenic) were identified using von Kossa and Oil Red O staining (Fig. 2b and d). qRT-PCR revealed that the expression of

osteogenic-specific markers (osteocalcin; OC and collagen type 1 alpha 1; COL1A1) was increased in differentiated PD-MSCs^{PRL-1} compared with that in undifferentiated ones (Fig. 2a). In addition, the expression of adipsin and peroxisome proliferator-activated receptor gamma (PPAR-γ), which are specific markers for adipocytes, was higher in differentiated cells than in undifferentiated cells (Fig. 2c). Furthermore, both types of PD-MSCs^{PRL-1} differentiated into endodermal lineage hepatocytes. ICG uptake was evaluated in lentiviral and non-viral AMAXA PD-MSCs^{PRL-1} (Fig. 2f) to determine whether these cells exhibited hepatocyte function. mRNA expression of hepatogenic-specific marker, which is albumin, was examined to confirm hepatogenic differentiation (Fig. 2e). The mRNA expression of mature hepatocyte markers, including albumin, was higher in non-viral AMAXA PD-MSCs^{PRL-1} than in lentiviral ones. These findings indicate that both types of PD-MSCs^{PRL-1} retain the ability to differentiate into mesoderm and endodermal lineage cells.

Effect of PRL-1-dependent migration ability through the Rho family

To analyze the effect of PRL-1 on the migration ability of PD-MSCs^{PRL-1}, we performed a migration assay with PD-MSCs^{PRL-1} using a Transwell insert system. The number of both types of migrated PD-MSCs^{PRL-1} was higher than that of naïve cells (Fig. 3a). In addition, the number of migrated naïve and PD-MSCs^{PRL-1} was significantly decreased when cocultured with siRNA-PRL-1 treatment (Fig. 3b). The mRNA expression of PRL-1 was increased in PD-MSCs^{PRL-1} compared with that in naïve as well as in RhoA and ROCK1-enhanced PD-MSCs^{PRL-1}. Alternatively, downregulated PRL-1 decreased migration ability (Fig. 3c). These findings suggest that PRL-1 may promote the enhancement of migration-related signals through the Rho family.

Improved mitochondrial respirational metabolic states of PD-MSCs^{PRL-1} regulate mitochondrial biogenesis

To analyze mitochondrial respiration in PD-MSCs^{PRL-1} according to both gene delivery systems, we used the XF Cell Mito Stress test to evaluate the impact of mitochondrial complex inhibitors (oligomycin, FCCP and rotenone/AA) on the electron transport chain (ETC). Based on the OCR and ECAR, PD-MSCs^{PRL-1} generated using both systems had a more energetic metabolic state than did naïve cells (Fig. 4a). Maximal respiration capacity, which may account for the capability of cells to respond to an energy demand, was increased in PD-MSCs^{PRL-1} compared to that in naïve. In particular, non-viral system based PD-MSCs^{PRL-1} showed significant improvement in this capacity (Fig. 4b). In whole cell lysates, ATP, the mitochondrial final product, was also relatively increased in PD-MSCs^{PRL-1} generated using both systems compared with that in naïve (Fig. 4c).

Interestingly, although naïve and PD-MSCs^{PRL-1} using lentiviral groups showed no differences, intracellular ATP production in live cells in the non-viral AMAXA system group markedly improved (Fig. 4d). mtDNA copy number was confirmed to isolate gDNA from naïve and PD-MSCs^{PRL-1} and investigate self-renewal ability through mitochondrial function. mtDNA copy number was higher in PD-

MSCs^{PRL-1} than in naïve (Fig. 4e). In particular, PD-MSCs^{PRL-1} in the AMAXA system group prominently had a higher mtDNA copy number. Production of L-lactate, the end product of glycolysis, was assayed. L-lactate levels decreased in PD-MSCs^{PRL-1} generated using both systems compared with those in naïve (Fig. 4f). In glycolysis, pyruvate that forms under aerobic conditions undergoes conversion to acetyl Co-A by pyruvate dehydrogenase (PDH). Although heat shock protein 60, which mediates protein folding after import into the mitochondria, and prohibitin 1 (PHB1), which exhibits membrane-bound ring complex expression, showed no differences, the protein expression of PDH was higher in enhanced PD-MSCs^{PRL-1} generated using both systems than in naïve. In mitochondria, to produce ATP, succinate dehydrogenase (SDHA), a key component in Complex II of the ETC, increased in PD-MSCs^{PRL-1} generated using lentiviral and non-viral systems. The expression of cytochrome c (cyt c) related to Complex 4 of the ETC and cyt c oxidase (COX10) also increased in PD-MSCs^{PRL-1}. In addition, through voltage-dependent anion channel (VDAC) located in the mitochondrial outer membrane, superoxide free radicals are rapidly converted to H_2O_2 by superoxide dismutase 1 (SOD1) in the aerobic system [33].

Although VDAC expression in PD-MSCs^{PRL-1} was markedly higher than that in naïve cells, SOD1 showed no differences (Fig. 4g). In mammals, improvement in aerobic metabolic capacity occurs through transcriptionally regulated mitochondrial biogenesis [34]. The major factors in biogenesis (PGC-1α, nuclear respiratory factor 1; NRF1 and mtTFA) were detected by mRNA levels. Although NRF1 expression showed no differences following downregulation of PRL-1, PGC-1α and mtTFA expression significantly decreased after PRL-1 knock-down (Fig. 4h). These results suggest that enhanced PRL-1 in PD-MSCs using both gene delivery systems may affect mitochondrial biogenesis, particularly PRL-1 induced by the non-viral AMAXA system, promoting cellular aerobic metabolism.

In vivo non-viral PD-MSCs^{PRL-1} alleviate liver fibrosis in a rat model with BDL

BDL is the most common model of cholestasis injury in rodents and results in inflammation, hepatocyte apoptosis and fibrosis [35]. To analyze the hepatic regeneration of PD-MSCs^{PRL-1} generated using a nonviral AMAXA system in the BDL model, we established an early cirrhotic model. Ten days after BDL, we distributed the animals into the following groups: normal control group (Con), the nontransplantation group (NTx), naïve PD-MSCs-transplantation group (TTx Naïve), and PD-MSCs^{PRL-1}-transplantation group (TTx PRL-1+) (Fig. 5a). To evaluate the intrahepatic distribution of transplanted cells, PKH67 + cells were identified among the vein and periportal fibrotic area in the liver sections of TTx naïve and PRL-1 + groups at 1 week (Fig. 5b). In comparison to normal control rats, livers in BDL-induced NTx group detected diffused bile ductular proliferation with loss of enlarged hepatocytes. Histopathological analysis determined that collagen fibrotic area was distinctly increased. Transplanted rats showed decreased Sirius red and Masson's trichrome-stained collagen fiber area, and their hepatocytes were partly replaced by ductules compared with the NTx group at 3 weeks (Fig. 5c). In particular, rats transplanted TTx PRL-1 + group significantly decreased quantification of the fibrotic area from Sirius red and Masson's trichrome staining in comparison with those in the transplanted TTx naïve group (Fig. 5d and e). These findings

indicate that administration of PD-MSCs^{PRL-1} induced by a non-viral AMAXA gene delivery system decreased liver fibrosis in a rat model with BDL.

PD-MSCs $^{PRL-1}$ using a non-viral system enhance hepatic function by regulating mitochondrial metabolism in a rat BDL model

To confirm hepatic function by PD-MSCs^{PRL-1} transplantation in BDL-injured rat liver, mRNA and protein expression of albumin increased in transplantation groups compared with the NTx group. In the TTx PRL-1 + group, albumin level was remarkably higher than TTx naïve at 1 week as well as human PRL-1 expression (Fig. 6a and b). In addition, increased serum levels of ALT, AST and TBIL and decreased albumin levels were confirmed in the NTx group compared to the Con group. Although TBIL levels in TTx PRL-1 + showed no differences compared with TTx naïve livers, the serum levels of ALT, AST, and albumin were markedly improved (Table 4). The protein expression of RhoA and ROCK1 was increased in the TTx groups compared with that in the NTx group. Interestingly, the TTx PRL-1 group showed significantly higher expression of CDK4 and Cyclin D1 than did the TTx naïve group (Fig. 6c).

Table 4
Improved liver functions according to MSC transplantation in rat serum levels of BDL model

	ALT (U/L)	AST (U/L)	TBIL (μmol/L)	Albumin (g/L)
Normal control (Con)	39.4 ± 3.6	97.1 ± 7.3	1.1 ± 0.3	34.4 ± 2.3
NTx	152.8 ± 7.2†	797.4 ± 32.0†	121.1 ± 4.8†	21.5 ± 0.5†
TTx (naïve)	125.6 ± 6.9†,*	690.9 ± 34.7†,*	96.5 ± 5.3†,*	24.2 ± 0.5†,*
TTx (PRL-1+)	104.0 ± 9.1$^{\dagger,*,\#}$	523.3 ± 34.0$^{\dagger,*,\#}$	101.4 ± 1.7†,*	27.0 ± 0.3$^{\dagger,*,\#}$

Each group was $n = 18$. Data are presented as mean ± SD. $^{\dagger}p < 0.05$ versus Con group; $^{*}p < 0.05$ versus NTx group; $^{\#}p < 0.05$ versus TTx naïve group. *ALT*; alanine aminotransferase, *AST*; aspartate aminotransferase, *Con*; control group, *TBIL*; total bilirubin

To demonstrate alterations in hepatic metabolism induced by PD-MSCs^{PRL-1} in BDL, the protein levels of mitochondrial metabolism-specific markers (PDH, SDHA, ATP5B, and PHB1) were significantly increased in the TTx PRL-1 + group compared with those in the NTx and TTx naïve groups (Fig. 6d). Moreover, mtDNA copy number and ATP production in the naïve transplantation group were higher than that in the NTx group. In particular, compared with the TTx naïve group, the TTx PRL-1 + group showed remarkably enhanced mtDNA copy number and ATP production (Fig. 6e and f). These findings indicate that PD-MSCs^{PRL-1} induced by a non-viral AMAXA gene delivery system may promote hepatic function by regulating mitochondrial metabolism in the liver.

PD-MSCs^{PRL-1} co-culture activate mitochondrial dynamics of primary hepatocytes

To demonstrate hepatic mitochondrial function, primary hepatocytes were isolated from rats and co-cultured with non-viral PD-MSCs^{PRL-1} in accordance with PRL-1 knockdown. In vitro modeling was induced by LCA treatment for the accumulation of bile acid. In advance, the protein expression of albumin in hepatocytes was decreased according to LCA treatment as well as PRL-1 expression. However, PD-MSCs^{PRL-1} co-culture recovered the expression of albumin and PRL-1 compared to naïve cells (Fig. 7a). To verify mitochondrial function of hepatocytes, although the protein expression of mitochondrial metabolism (PDH and ATP5B) decreased with LCA treatment, naïve PD-MSCs co-culture was slightly increased. Interestingly, PDH and ATP5B levels in PD-MSCs^{PRL-1} co-culture were higher than in naïve cells (Fig. 7b). In addition, mRNA levels of PGC-1α, NRF1, and mtTFA, which is a key factor of mitochondrial dynamics, showed decreased levels in LCA treatment group. However, PD-MSCs^{PRL-1} co-culture significantly improved gene expression (Fig. 7c). mRNA and protein expression was PRL-1-dependent. While mtDNA copy number and ATP production in primary hepatocytes receiving LCA treatment were reduced, PD-MSCs^{PRL-1} co-culture had a significant increase compared to naïve cells (Fig. 7d and e). These data suggest that PD-MSCs^{PRL-1} may stimulate improved mitochondrial metabolism in primary hepatocytes.

Discussion

As an alternative to liver transplantation, MSC-based therapy for regenerative medicine has been attempted for the treatment of various liver diseases, including hepatic failure and liver cirrhosis [36, 37]. According to our previous reports, PD-MSCs have antifibrotic effects by increased MMP activities as well as hepatic regeneration in a CCl_4-injured rat model via an increased autophagic mechanism [32]. Recently, researchers have attempted clinical trials in patients with alcoholic hepatic cirrhosis using autologous BM-MSCs. In phase I and II clinical trials, Jang and their colleagues reported that BM-MSCs were primarily safe and that the autologous BM-MSCs had antifibrotic effects for patients with alcoholic hepatic cirrhosis [38]. Nevertheless, clinical applications of BM-MSCs have been hampered by several weaknesses, including a painful isolation procedure for patients, a lack of fresh cells, high price and lack of understanding of the therapeutic mechanism [39]. The production of functionally enhanced MSCs with therapeutic efficacy-enhancing factors and verification of therapeutic efficacy are emerging to overcome these limitations of MSC-based cell therapy.

Recently, PRL-1 has been shown to play an important role in cell cycle progression during hepatic regeneration [27]. However, the effect of PRL-1 on PD-MSC properties remains poorly understood. In our study, we demonstrated that PRL-1-overexpressing PD-MSCs (PD-MSCs^{PRL-1}, PRL-1+) were successfully generated using lentiviral and non-viral AMAXA gene delivery systems and analyzed their characteristics, which were similar to those of naïve cells (Figs. 1 and 2). Interestingly, the mitochondrial respirational metabolic state and cellular aerobic metabolism significantly increased in PD-MSCs^{PRL-1} in both gene delivery systems. In particular, mtDNA synthesis and mitochondrial biogenesis were remarkably enhanced by PRL-1 in the non-viral AMAXA system, and ATP production in mitochondria in live cellular conditions also increased, maintaining an energetic state (Fig. 4). Although differences in cellular

mitochondrial mechanisms according to gene delivery systems have remained unclear, viral systems carry a possible risk of cancer and immunologic side effects [40].

In general, MSCs genetically engineered by viral gene delivery systems have important safety issues, such as the genomic instability of the cells. For this reason, many researchers have attempted to produce stem cells with enhanced function based on non-viral gene delivery systems, such as AMAXA systems, and have also applied them to clinical trials using enhanced functional stem cells. In the present study, PD-MSCs^{PRL-1}, which are enhanced functional PD-MSCs, were generated using non-viral AMAXA systems, and no teratoma formation occurred when these cells were transplanted into the testes of NOD/SCID mice. Our studies revealed that compared with naïve PD-MSC transplantation, non-viral PD-MSC^{PRL-1} transplantation remarkably enhanced engraftment in the injured target organs through the activated Rho family and albumin synthesis (Fig. 6). These data are similar to previous studies demonstrating that PRL-1 binding to p115 Rho GAP promotes ERK1/2 and RhoA activation [24].

Mitochondria-meditated function is associated with liver regeneration [41]. In chronic cholestasis, mitochondrial dysfunction, associated with decreased activities of respiratory chain complexes, mitochondrial membrane potential and ATP production, was characterized [42]. The lack of stimulation of mitochondrial biogenesis in a rat BDL model leads to severe depletions and deletions of mtDNA copy number [43]. Additionally, hepatic injury caused by cholestasis affects oxidative stress in mitochondria in the liver. PGC-1α and mtTFA are impaired in the BDL model [44]. By transplantation of MSCs, hepatic mitochondrial dysfunctions are reversed by mediating the nuclear factor erythroid-derived 2-related factor 2(Nrf2)/HO1 pathway [45]. The effects of MSCs are due to the more rapid recovery of the number of mitochondria and the function of hepatic mitochondria [46]. These previous reports support our conclusion that mtDNA and ATP synthesis are increased in liver tissues during liver regeneration following transplantation of functionally enhanced PD-MSCs. Additionally, we recently reported that mitochondrial energy metabolism following cellular ATP production was restored by naïve PD-MSC transplantation in a cholestatic liver disease model [47]. Our data elucidated that compared with naïve PD-MSCs, PD-MSCs^{PRL-1} generated using non-viral AMAXA system transplantation promoted mtDNA synthesis. Additionally, to promote hepatic ATP production, PDH and SDHA are more activated in hepatic mitochondrial ETC in PD-MSCs^{PRL-1} compared with those in naïve cells. Finally, hepatic ATP production was enhanced by PD-MSCs^{PRL-1} generated using non-viral AMAXA system transplantation in a rat BDL model as well as primary hepatocytes (Figs. 7 and 8). Transplantation of PD-MSCs with PRL-1 using a non-viral AMAXA system in a rat hepatic disease model established with BDL promotes hepatic functions by upregulating mitochondrial metabolism.

Conclusion

In conclusion, PD-MSCs^{PRL-1} generated using the non-viral AMAXA system impacted mitochondrial respirational metabolic states more than those generated using the lentiviral-based gene delivery system. In particular, the therapeutic effects of PD-MSCs^{PRL-1} using non-viral AMAXA system transplantation

accelerate liver function by promoting mitochondrial metabolism (Fig. 8). These findings provide novel insights into next-generation MSC-based cell therapy, including safe gene modification, and useful data for therapeutic strategies using PD-MSCs for regenerative medicine in liver disease.

Abbreviations

AA: Antimycin A; ALT: alanine aminotransferase; α-MEM: Alpha-modified minimal essential medium; AST: aspartate aminotransferase; BDL: Bile duct ligation; bFGF: Basic fibroblast growth factor; BM-MSCs: Bone marrow-derived mesenchymal stem cell; CCl_4: Carbon tetrachloride; CD: Cluster of differentiation; COL1A1: Collagen type 1 alpha 1; COX10: Cytochrome c oxidase; Cyt c: Cytochrome c; DAPI: 4',6-diamidino-2-phenylindole; DMEM: Dulbecco's-modified Eagle medium; ECAR: Extracellular acidification rate; EGF: Epidermal growth factor; Egr-1: Early growth response factor-1; ETC: Electron transport chain; FBS: Fetal bovine serum; FCCP: Carbonyl cyanide-*p*-trifluoromethoxyphenylhydrazone; GAPDH: Glyceraldehyde 3-phosphate dehydrogenase; gDNA: Genomic DNA; GFP: Green fluorescent protein; hFGF-4: Human fibroblast growth factor-4; H&E: Hematoxylin & eosin; HLA: Human leukocyte antigen; HO: Heme oxygenase; ICG: Indocyanine green; IL-6: Interleukin-6; IRB: Institutional Review Board; MMP: Matrix metalloproteinase; mtDNA: Mitochondrial DNA; mtTFA: Mitochondrial transcription factor A; NBF: neutral buffered formalin; NOD/SCID: Nonobese diabetic/severe combined immunodeficiency; NRF1: Nuclear respiratory factor 1; Nrf2: Nuclear factor erythroid-derived 2-related factor 2; OC: Osteocalcin; OCR: Oxygen consumption rate; PDH: Pyruvate dehydrogenase; PD-MSCs: Placenta-derived mesenchymal stem cells; PGC-1α: Peroxisome proliferator-activated receptor-gamma coactivator-1 alpha; PHB1: Prohibitin 1; PPAR-γ: Peroxisome proliferator-activated receptor gamma; PRL-1: Phosphatase of regenerating liver-1; P/S: Penicillin/streptomycin; PTP4A1: Protein tyrosine phosphatase type 4 A, member 1; SD: Sprague-Dawley; SDHA: Succinate dehydrogenase; SOD1: Superoxide dismutase 1; STAT3: signal transducer and activator of transcription 3; TBIL: total bilirubin; TERT: Telomerase reverse transcriptase; VDAC: Voltage-dependent anion channel

Declarations

Ethics approval and consent to participate

The animal experiments were approved by the Institutional Review Board (IRB) of CHA General Hospital, Seoul, Korea (IACUC-180023). The collection of placenta samples and their use for research purposes were approved by the IRB of CHA General Hospital, Seoul, Korea (IRB 07-18).

Consent for publication

Not applicable.

Availability of data and material

All data analyzed for this study are included in this article.

Competing interests

The authors declare that they have no competing interests.

Funding

This research was supported by a grant of the Korea Health Technology R&D Project through the Korea Health Industry Development Institute (KHIDI), funded by the Ministry of Health & Welfare, Republic of Korea (HI17C1050) and by Basic Science Research Program through the National Research Foundation of Korea (NRF) funded by the Ministry of Education, Science and Technology (2020M3A9B3026182)..

Authors' contributions

JYK did analysis and interpretation of data, and manuscript drafting, JHC and JHJ did analysis and collection of data, SP and JJ did interpretation of data and manuscript drafting. SHB helped critical discussion. GJK conceived and designed the experiments, and directed manuscript drafting, financial support and final approval of manuscript.

Author details

[1]Department of Biomedical Science, CHA University, Seongnam, 13488, Republic of Korea; [2]Department of Oral Pathology, College of Dentistry, Gangneung-Wonju National University, Gangneung, 25457, Republic of Korea; [3]Department of Internal Medicine, Catholic University Medical College, Seoul, 06591, Republic of Korea

References

1. Volarevic V, Nurkovic J, Arsenijevic N, Stojkovic M. Concise review: Therapeutic potential of mesenchymal stem cells for the treatment of acute liver failure and cirrhosis. Stem Cells.

2014;32(11):2818–23.

2. Weng J, Li W, Jia X, An W. Alleviation of Ischemia-Reperfusion Injury in Liver Steatosis by Augmenter of Liver Regeneration Is Attributed to Antioxidation and Preservation of Mitochondria. Transplantation. 2017;101(10):2340–8.
3. Sastre J, Serviddio G, Pereda J, Minana JB, Arduini A, Vendemiale G, Poli G, Pallardo FV, Vina J. Mitochondrial function in liver disease. Front Biosci. 2007;12:1200–9.
4. Perez-Carreras M, Del Hoyo P, Martin MA, Rubio JC, Martin A, Castellano G, Colina F, Arenas J, Solis-Herruzo JA. Defective hepatic mitochondrial respiratory chain in patients with nonalcoholic steatohepatitis. Hepatology. 2003;38(4):999–1007.
5. Valdecantos MP, Pardo V, Ruiz L, Castro-Sanchez L, Lanzon B, Fernandez-Millan E, et al. A novel glucagon-like peptide 1/glucagon receptor dual agonist improves steatohepatitis and liver regeneration in mice. Hepatology. 2017;65(3):950–68.
6. Han LH, Dong LY, Yu H, Sun GY, Wu Y, Gao J, Thasler W, An W. Deceleration of liver regeneration by knockdown of augmenter of liver regeneration gene is associated with impairment of mitochondrial DNA synthesis in mice. Am J Physiol Gastrointest Liver Physiol. 2015;309(2):G112-22.
7. Cai Y, Zou Z, Liu L, Chen S, Chen Y, Lin Z, Shi K, Xu L, Chen Y. Bone marrow-derived mesenchymal stem cells inhibits hepatocyte apoptosis after acute liver injury. Int J Clin Exp Pathol. 2015;8(1):107–16.
8. Kallis YN, Alison MR, Forbes SJ. Bone marrow stem cells and liver disease. Gut. 2007;56(5):716–24.
9. Zhang Z, Wang FS. Stem cell therapies for liver failure and cirrhosis. J Hepatol. 2013;59(1):183–5.
10. Jin S, Li H, Han M, Ruan M, Liu Z, Zhang F, Zhang C, Choi Y, Liu B. Mesenchymal Stem Cells with Enhanced Bcl-2 Expression Promote Liver Recovery in a Rat Model of Hepatic Cirrhosis. Cell Physiol Biochem. 2016;40(5):1117–28.
11. Pankaj P, Zhang Q, Bai XL, Liang TB. Autologous bone marrow transplantation in decompensated liver: Systematic review and meta-analysis. World J Gastroenterol. 2015;21(28):8697–710.
12. Ma XR, Tang YL, Xuan M, Chang Z, Wang XY, Liang XH. Transplantation of autologous mesenchymal stem cells for end-stage liver cirrhosis: a meta-analysis based on seven controlled trials. Gastroenterol Res Pract. 2015;2015:908275.
13. Pan XN, Zheng LQ, Lai XH. Bone marrow-derived mesenchymal stem cell therapy for decompensated liver cirrhosis: a meta-analysis. World J Gastroenterol. 2014;20(38):14051–7.
14. Suk KT, Yoon JH, Kim MY, Kim CW, Kim JK, Park H, et al. Transplantation with autologous bone marrow-derived mesenchymal stem cells for alcoholic cirrhosis: Phase 2 trial. Hepatology. 2016;64(6):2185–97.
15. Mohamadnejad M, Namiri M, Bagheri M, Hashemi SM, Ghanaati H, Zare Mehrjardi N, Kazemi Ashtiani S, Malekzadeh R, Baharvand H. Phase 1 human trial of autologous bone marrow-hematopoietic stem cell transplantation in patients with decompensated cirrhosis. World J Gastroenterol. 2007;13(24):3359–63.

16. Fukuchi Y, Nakajima H, Sugiyama D, Hirose I, Kitamura T, Tsuji K. Human placenta-derived cells have mesenchymal stem/progenitor cell potential. Stem Cells. 2004;22(5):649–58.
17. Abumaree MH, Abomaray FM, Alshabibi MA, AlAskar AS, Kalionis B. Immunomodulatory properties of human placental mesenchymal stem/stromal cells. Placenta. 2017;59:87–95.
18. Jung J, Choi JH, Lee Y, Park JW, Oh IH, Hwang SG, Kim KS, Kim GJ. Human placenta-derived mesenchymal stem cells promote hepatic regeneration in CCl4 -injured rat liver model via increased autophagic mechanism. Stem Cells. 2013;31(8):1584–96.
19. Jung J, Moon JW, Choi JH, Lee YW, Park SH, Kim GJ. Epigenetic Alterations of IL-6/STAT3 Signaling by Placental Stem Cells Promote Hepatic Regeneration in a Rat Model with CCl4-induced Liver Injury. Int J Stem Cells. 2015;8(1):79–89.
20. Hyun J, Wang S, Kim J, Kim GJ, Jung Y. MicroRNA125b-mediated Hedgehog signaling influences liver regeneration by chorionic plate-derived mesenchymal stem cells. Sci Rep. 2015;5:14135.
21. Yu J, Hao G, Wang D, Liu J, Dong X, Sun Y, et al. Therapeutic Effect and Location of GFP-Labeled Placental Mesenchymal Stem Cells on Hepatic Fibrosis in Rats. Stem Cells Int. 2017;2017:1798260.
22. Rios P, Li X, Kohn M. Molecular mechanisms of the PRL phosphatases. FEBS J. 2013;280(2):505–24.
23. Mueller L, Broering DC, Meyer J, Vashist Y, Goettsche J, Wilms C, Rogiers X. The induction of the immediate-early-genes Egr-1, PAI-1 and PRL-1 during liver regeneration in surgical models is related to increased portal flow. J Hepatol. 2002;37(5):606–12.
24. Bai Y, Luo Y, Liu S, Zhang L, Shen K, Dong Y, et al. PRL-1 protein promotes ERK1/2 and RhoA protein activation through a non-canonical interaction with the Src homology 3 domain of p115 Rho GTPase-activating protein. J Biol Chem. 2011;286(49):42316–24.
25. Luo Y, Liang F, Zhang ZY. PRL1 promotes cell migration and invasion by increasing MMP2 and MMP9 expression through Src and ERK1/2 pathways. Biochemistry. 2009;48(8):1838–46.
26. Nakashima M, Lazo JS. Phosphatase of regenerating liver-1 promotes cell migration and invasion and regulates filamentous actin dynamics. J Pharmacol Exp Ther. 2010;334(2):627–33.
27. Jiao Y, Ye DZ, Li Z, Teta-Bissett M, Peng Y, Taub R, Greenbaum LE, Kaestner KH. Protein tyrosine phosphatase of liver regeneration-1 is required for normal timing of cell cycle progression during liver regeneration. Am J Physiol Gastrointest Liver Physiol. 2015;308(2):G85–91.
28. Kobayashi M, Chen S, Gao R, Bai Y, Zhang ZY, Liu Y. Phosphatase of regenerating liver in hematopoietic stem cells and hematological malignancies. Cell Cycle. 2014;13(18):2827–35.
29. Kobayashi M, Bai Y, Dong Y, Yu H, Chen S, Gao R, et al. PRL2/PTP4A2 phosphatase is important for hematopoietic stem cell self-renewal. Stem Cells. 2014;32(7):1956–67.
30. Kim MJ, Shin KS, Jeon JH, Lee DR, Shim SH, Kim JK, Cha DH, Yoon TK, Kim GJ. Human chorionic-plate-derived mesenchymal stem cells and Wharton's jelly-derived mesenchymal stem cells: a comparative analysis of their potential as placenta-derived stem cells. Cell Tissue Res. 2011;346(1):53–64.

31. Kountouras J, Billing BH, Scheuer PJ. Prolonged bile duct obstruction: a new experimental model for cirrhosis in the rat. Br J Exp Pathol. 1984;65(3):305–11.
32. Lee MJ, Jung J, Na KH, Moon JS, Lee HJ, Kim JH, et al. Anti-fibrotic effect of chorionic plate-derived mesenchymal stem cells isolated from human placenta in a rat model of CCl(4)-injured liver: potential application to the treatment of hepatic diseases. J Cell Biochem. 2010;111(6):1453–63.
33. Madesh M, Hajnoczky G. VDAC-dependent permeabilization of the outer mitochondrial membrane by superoxide induces rapid and massive cytochrome c release. J Cell Biol. 2001;155(6):1003–15.
34. O'Brien KM. Mitochondrial biogenesis in cold-bodied fishes. J Exp Biol. 2011;214(Pt 2):275–85.
35. Eguchi A, Koyama Y, Wree A, Johnson CD, Nakamura R, Povero D, et al. Emricasan, a pan-caspase inhibitor, improves survival and portal hypertension in a murine model of common bile-duct ligation. J Mol Med (Berl). 2018;96(6):575–83.
36. Gazdic M, Arsenijevic A, Markovic BS, Volarevic A, Dimova I, Djonov V, Arsenijevic N, Stojkovic M, Volarevic V. Mesenchymal Stem Cell-Dependent Modulation of Liver Diseases. Int J Biol Sci. 2017;13(9):1109–17.
37. Fiore EJ, Mazzolini G, Aquino JB. Mesenchymal Stem/Stromal Cells in Liver Fibrosis: Recent Findings, Old/New Caveats and Future Perspectives. Stem Cell Rev. 2015;11(4):586–97.
38. Jang YO, Kim YJ, Baik SK, Kim MY, Eom YW, Cho MY, et al. Histological improvement following administration of autologous bone marrow-derived mesenchymal stem cells for alcoholic cirrhosis: a pilot study. Liver Int. 2014;34(1):33–41.
39. Eom YW, Shim KY, Baik SK. Mesenchymal stem cell therapy for liver fibrosis. Korean J Intern Med. 2015;30(5):580–9.
40. Cizkova D, Cubinkova V, Smolek T, Murgoci AN, Danko J, Vdoviakova K, et al Correction: Cizkova D, et al. Localized Intrathecal Delivery of Mesenchymal Stromal Cells Conditioned Media Improves Functional Recovery in A Rat Model of Contusive Spinal Cord Injury. Int. J. Mol. Sci. 2018, 19, 870. Int J Mol Sci. 2018;19(7).
41. Buckle M. Regulation of ATP hydrolase activity of the F0-F1 complex of rat-liver mitochondria during early hepatic regeneration. FEBS Lett. 1986;209(2):197–202.
42. Serviddio G, Pereda J, Pallardo FV, Carretero J, Borras C, Cutrin J, et al. Ursodeoxycholic acid protects against secondary biliary cirrhosis in rats by preventing mitochondrial oxidative stress. Hepatology. 2004;39(3):711–20.
43. Arduini A, Serviddio G, Escobar J, Tormos AM, Bellanti F, Vina J, Monsalve M, Sastre J. Mitochondrial biogenesis fails in secondary biliary cirrhosis in rats leading to mitochondrial DNA depletion and deletions. Am J Physiol Gastrointest Liver Physiol. 2011;301(1):G119-27.
44. Tiao MM, Lin TK, Wang PW, Chen JB, Liou CW. The role of mitochondria in cholestatic liver injury. Chang Gung Med J. 2009;32(4):346–53.
45. Yan W, Li D, Chen T, Tian G, Zhou P, Ju X. Umbilical Cord MSCs Reverse D-Galactose-Induced Hepatic Mitochondrial Dysfunction via Activation of Nrf2/HO-1 Pathway. Biol Pharm Bull. 2017;40(8):1174–82.

46. El'chaninov AV, Volodina MA, Arutyunyan IV, Makarov AV, Tarasova NV, Kananykhina EY, et al. Effect of multipotent stromal cells on the function of cell mitochondria in regenerating liver. Bull Exp Biol Med. 2015;158(4):566–72.
47. Lee YB, Choi JH, Kim EN, Seok J, Lee HJ, Yoon JH, Kim GJ. Human Chorionic Plate-Derived Mesenchymal Stem Cells Restore Hepatic Lipid Metabolism in a Rat Model of Bile Duct Ligation. Stem Cells Int. 2017;2017:5180579.

Figures

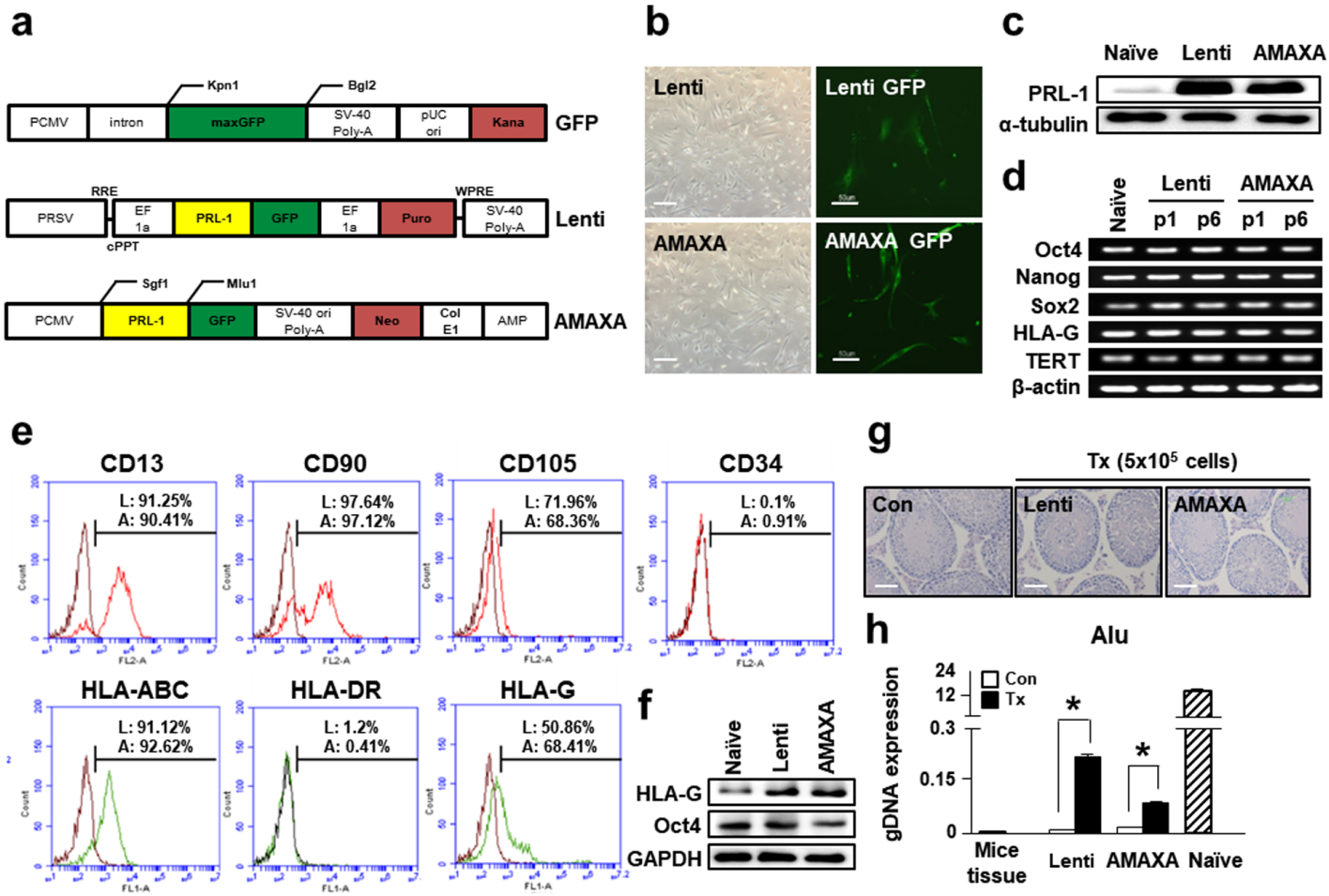

Figure 1

Generation of stable PD-MSCs with PRL-1 (PD-MSCsPRL-1, PRL-1+) using lentiviral and non-viral AMAXA systems. a GFP, lentiviral, and non-viral AMAXA plasmid vector map. b Morphology of PD-MSCsPRL-1 using lentiviral and non-viral AMAXA systems. Scale bars = 100 μm. The expression of GFP into PD-MSCs after each transfection system. Scale bars = 50 μm. c Western blotting of PRL-1 expression in naïve and PD-MSCsPRL-1. d RT-PCR analysis of stemness markers in naïve and PD-MSCsPRL-1 depend on passages. e FACS analysis of surface markers related to hematopoietic, non-hematopoietic and HLA-family in PD-MSCsPRL-1. f Western blotting of Oct4 and HLA-G expression in naïve and PD-MSCsPRL-1.

g H&E staining of the normal and PD-MSCsPRL-1 transplanted NOD/SCID mice testis post 14 weeks (lenti; n = 2, AMAXA; n = 2). Scale bars = 50 μm. h Engraftment of PD-MSCsPRL-1 into mice testis post-transplantation. Mouse tissue was used as a negative control. Human PD-MSCs were used as a positive control. Data from each group are expressed as mean ± SD. *p < 0.05 versus Con group. Con; control, GAPDH; glyceraldehyde 3-phosphate dehydrogenase, GFP; green fluorescent protein, PRL-1; phosphatase of regenerating liver-1, TERT; telomerase reverse transcriptase

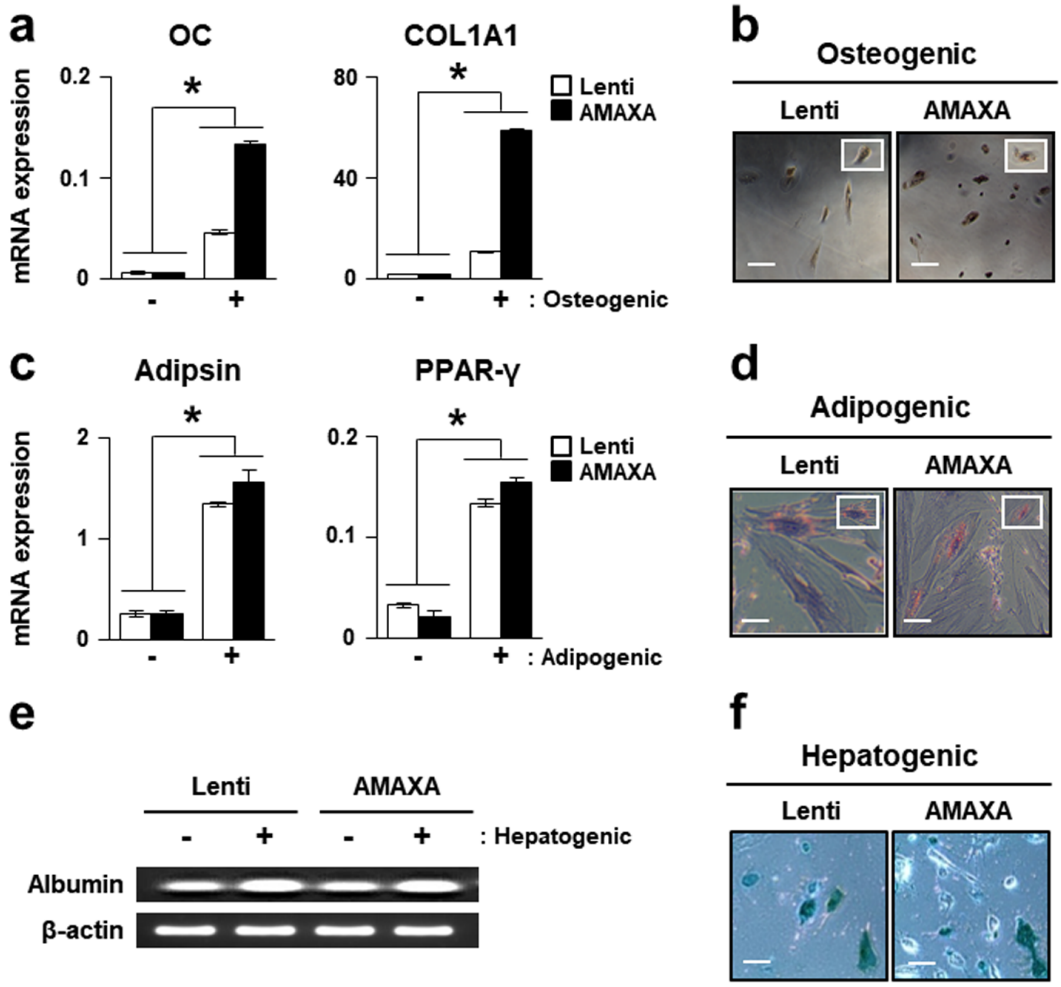

Figure 2

Multidifferentiation potential of PD-MSCsPRL-1. a qRT-PCR analysis of osteogenic markers (OC and COL1A1) in undifferentiated and differentiated PD-MSCsPRL-1. b Von Kossa staining in osteogenic differentiation of PD-MSCsPRL-1. Scale bars = 50 μm. c qRT-PCR analysis of adipogenic markers (Adipsin and PPAR-γ) in undifferentiated and differentiated PD-MSCsPRL-1. d Oil Red O staining in adipogenic differentiation of PD-MSCsPRL-1. Scale bars = 50 μm. e RT-PCR analysis of the hepatocyte function marker albumin in undifferentiated and differentiated PD-MSCsPRL-1. f ICG uptake in PD-MSCsPRL-1 after hepatogenic differentiation. Scale bars = 50 μm. Data from each group are expressed as mean ± SD. *p < 0.05 versus undifferentiated group. COL1A1; collagen type 1 alpha 1, OC; osteocalcin, PPAR-γ; peroxisome proliferator-activated receptor gamma

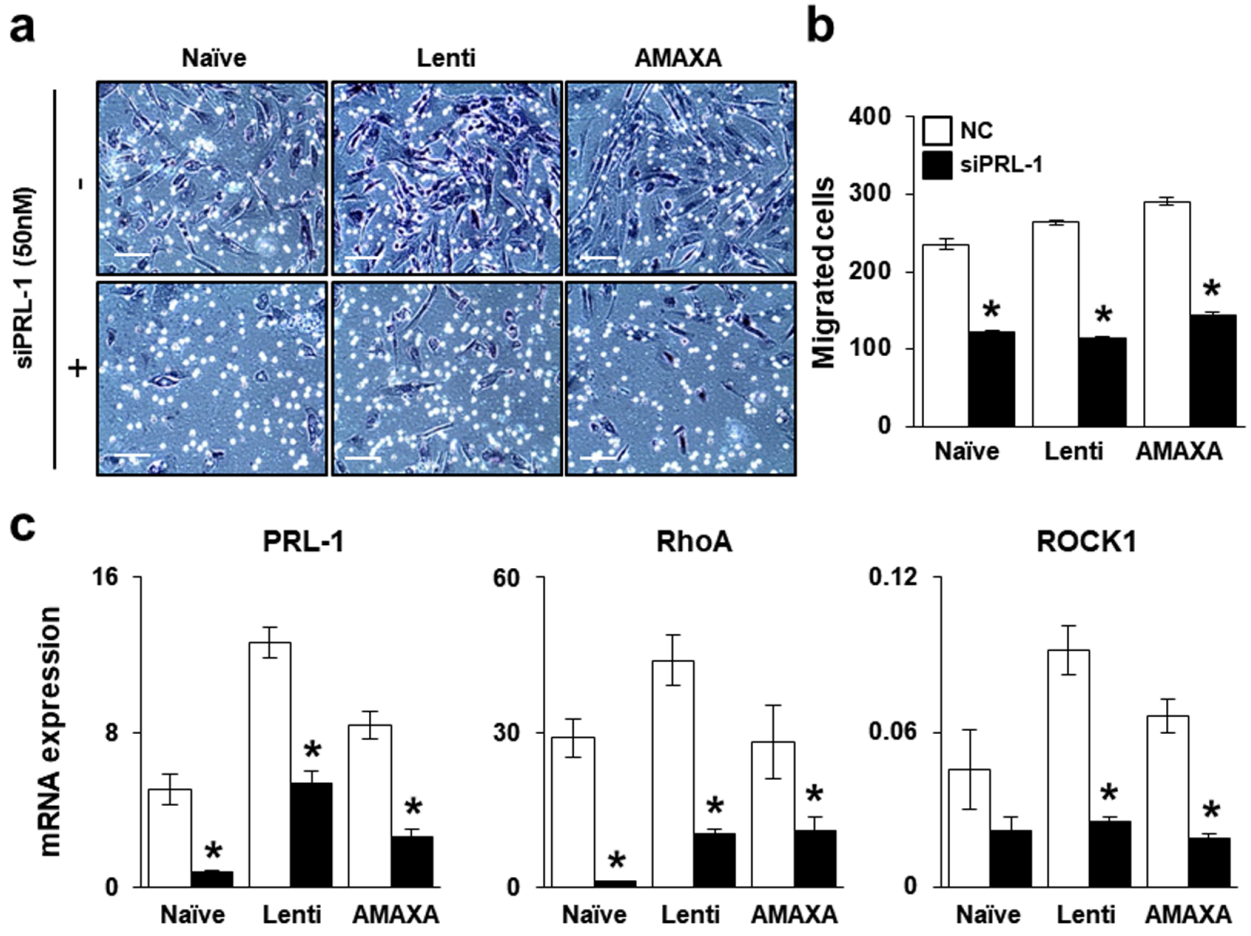

Figure 3

Effect of PRL-1-dependent migration ability through the Rho family. a, b Representative images and quantification of migrated naïve and PD-MSCsPRL-1 in a Transwell insert system treated or untreated with siRNA-PRL-1 (50 nM) after 24 h. Scale bars = 100 μm. c qRT-PCR analysis of mRNA PRL-1 and Rho family (RhoA and ROCK1) expression in migrated naïve and PD-MSCsPRL-1 from upper chamber to the lower chamber after treatment with or without siRNA-PRL-1. Data from each group are expressed as mean ± SD. *p < 0.05 versus NC, PRL-1; phosphatase of regenerating liver-1

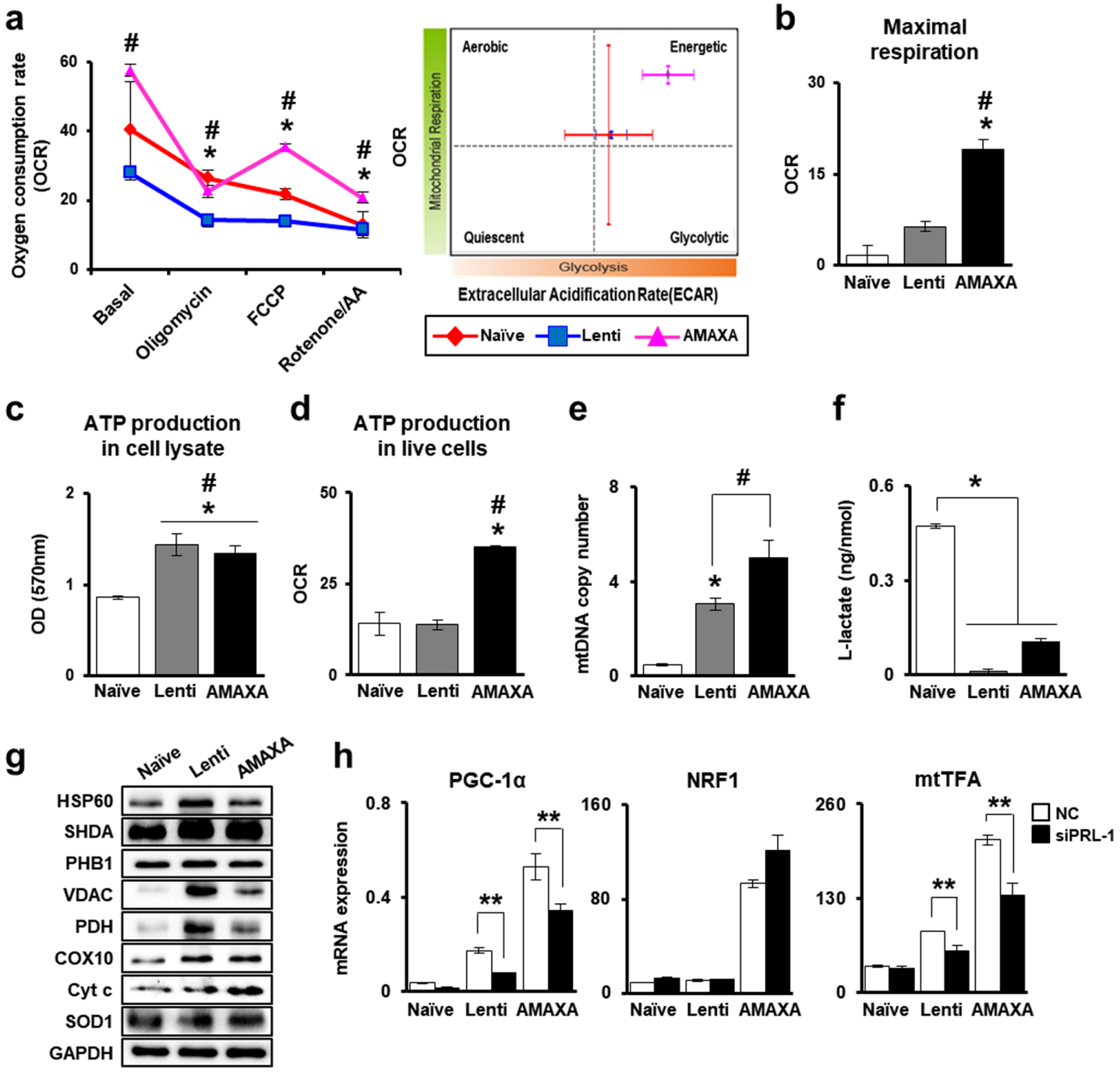

Figure 4

Improved mitochondrial respirational metabolic states of PD-MSCsPRL-1 regulate mitochondrial dynamics. a OCR and ECAR of PD-MSCsPRL-1 using lentiviral and non-viral AMAXA systems after sequential treatment with 1 μM oligomycin, 0.5 μM FCCP and 0.5 μM rotenone/AA by Seahorse XF24 analyzer. Quantification of b maximal respiration and d ATP production under live conditions of naïve and PD-MSCsPRL-1. c ATP production assay in naïve and PD-MSCsPRL-1 lysate (10 μg/μl). e mtDNA copy number of PD-MSCsPRL-1 using lentiviral and non-viral AMAXA systems by taqman assay. Human nuclear DNA was used as an internal control. f L-lactate production assay of PD-MSCsPRL-1 using cell

lysate (<25 mg/ml). g Western blotting of mitochondrial metabolism-specific genes in naïve and PD-MSCsPRL-1. h qRT-PCR analysis of mitochondrial biogenesis specific genes (PGC-1α, NRF1, and mtTFA) in PD-MSCsPRL-1 treated or untreated siRNA-PRL-1 (50 nM) after 24 h. Data from each group are shown as mean ± SD. *p < 0.05 versus naïve; #p < 0.05 versus lenti; **p < 0.05 versus NC. AA; antimycin A, COX10; cytochrome c oxidase 10, Cyt c; cytochrome c, ECAR; extracellular acidification rate, FCCP; carbonyl cyanide-p-trifluoromethoxyphenylhydrazone, GAPDH; glyceraldehyde 3-phosphate dehydrogenase, HSP60; heat shock protein 60, mtTFA; mitochondrial transcription factor A, NC; negative control, NRF1; nuclear respiratory factor 1, OCR; oxygen consumption rate, PDH; pyruvate dehydrogenase, PGC-1α; peroxisome proliferator-activated receptor-gamma coactivator-1 alpha, PHB1; prohibitin 1, SDHA; succinate dehydrogenase, SOD1; superoxide dismutase 1, VDAC; voltage-dependent anion channel

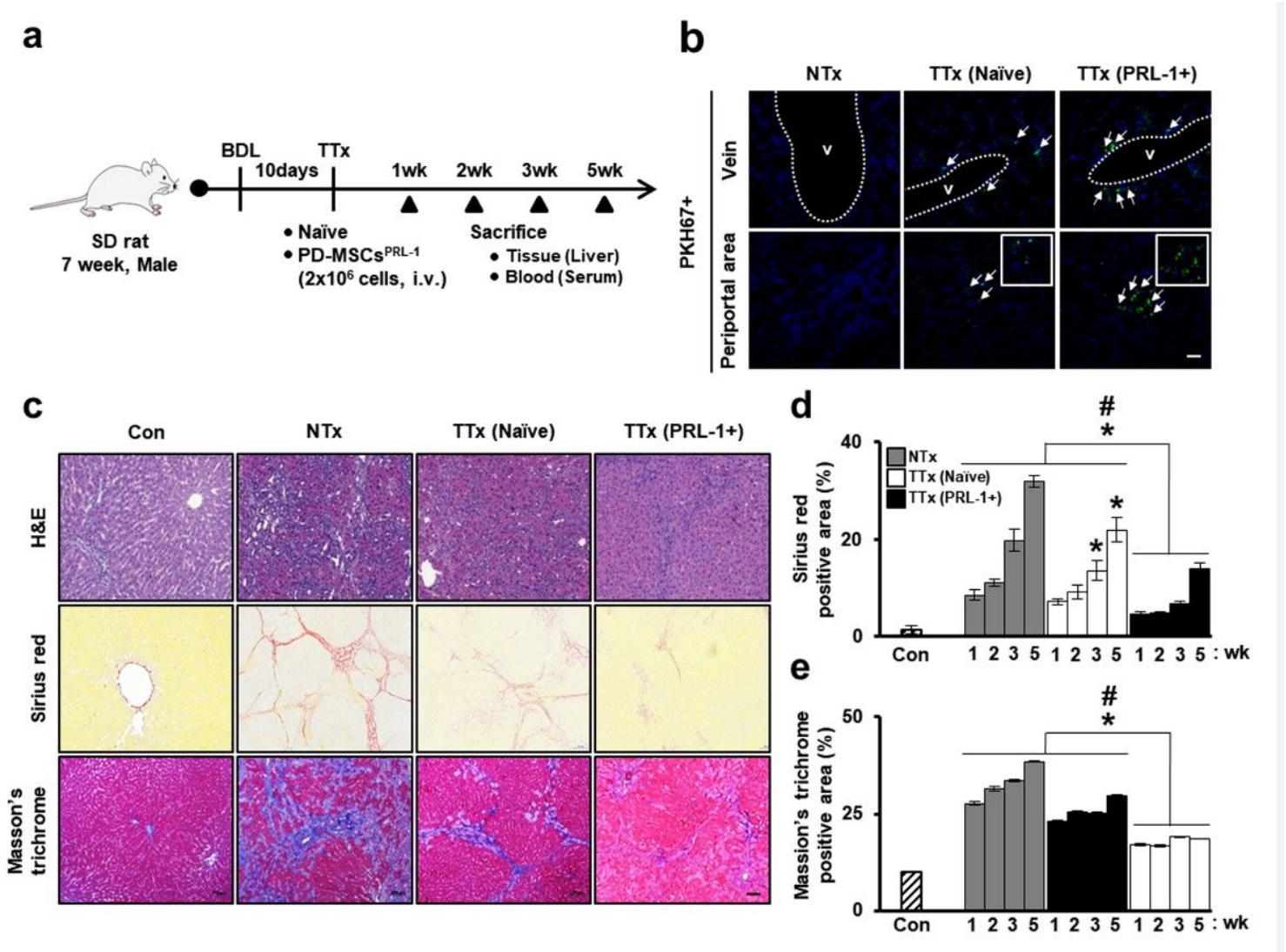

Figure 5

In vivo non-viral PD-MSCsPRL-1 alleviate liver fibrosis in a rat model with BDL. a A schematic diagram describing the rat BDL model (NTx; n = 20, TTx Naïve; n = 20, TTx PRL-1+; n = 20) as well as shame controls (Con; n = 5). b Engraftment of PKH67 (green) labeled with transplanted cells as injured rat liver by fluorescence microscopy at 1 week (arrow: PKH67+ signals) (green: PKH67; blue: DAPI). Scale bars =

100 μm. c Representative images of histopathological analysis in rat liver sections stained with H&E, Sirius red, and Masson's trichrome after naïve and PD-MSCPRL-1 transplantation at 3 week. Scale bars = 100 μm. Quantification of d Sirius red and e Masson's trichrome positive areas at 1, 2, 3, and 5 week in stained liver slides (n = 5). Data from each group are presented as mean ± SD. *p < 0.05 versus NTx group; #p < 0.05 versus TTx naïve group. BDL; bile duct ligation, Con; control group, H&E; hematoxylin & eosin, NTx; non-transplantation group, PRL-1; phosphatase of regenerating liver-1, TTx; transplantation group

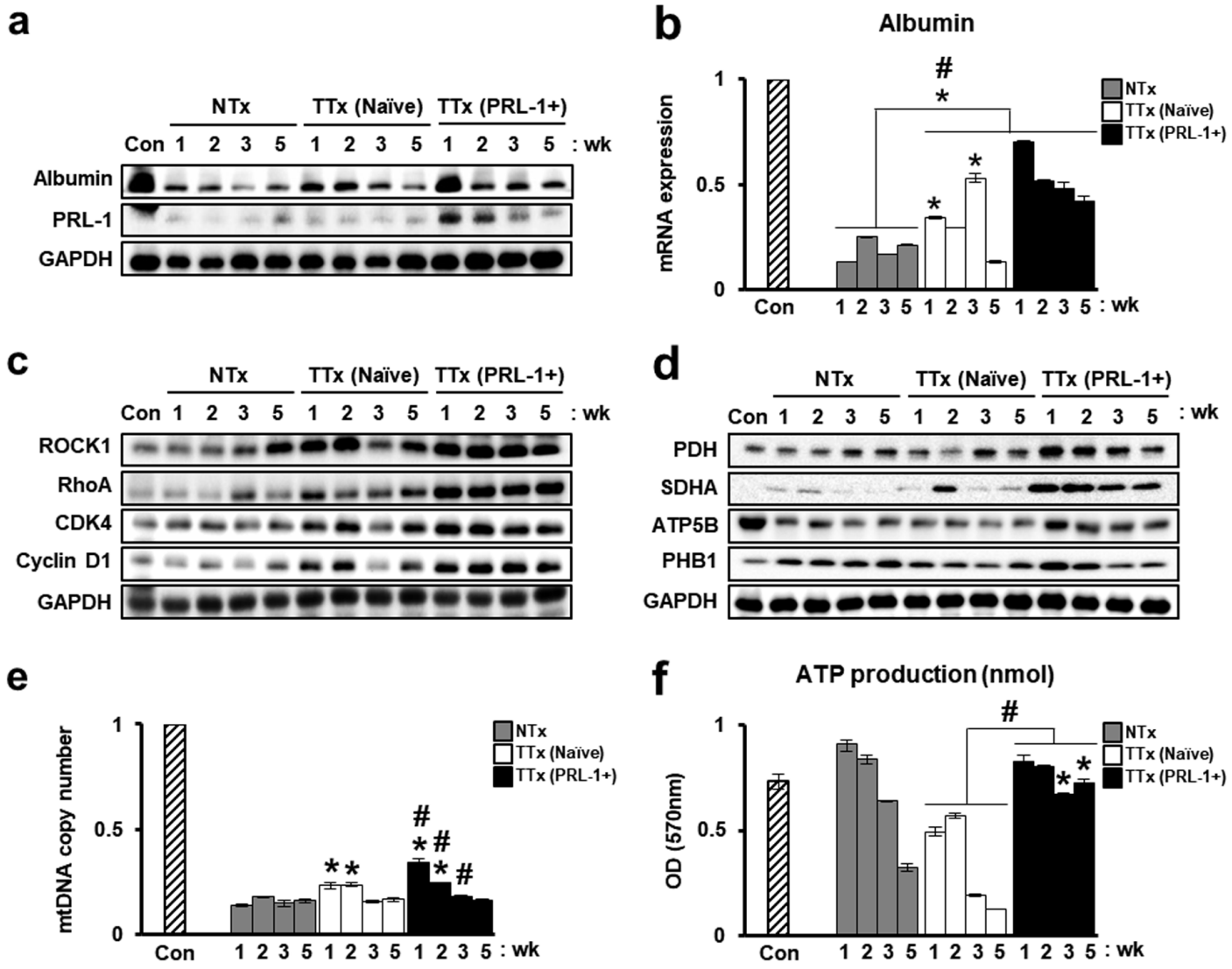

Figure 6

PD-MSCsPRL-1 using a non-viral system enhance hepatic function by regulating mitochondrial metabolism in a rat BDL model. a Western blotting of albumin, human PRL-1 genes expression by PD-MSCsPRL-1 transplantation in pooled BDL-injured rat liver tissue (n = 5). b mRNA expression of albumin in rat model with pooled BDL liver tissue (n = 5). Protein expression of c Rho family (ROCK1 and RhoA), cell cycle (CDK4 and Cyclin D1), and mitochondrial metabolism (PDH, SDHA, ATP5B, and PHB1) by PD-MSCsPRL-1 transplantation in pooled BDL-injured rat liver tissue (n = 5). e mtDNA copy number in BDL-

injured rat liver tissue by taqman assay. Rat nuclear DNA was used as an internal control. f ATP production assay in rat BDL liver lysate (10 μg/μl). Data from each group are presented as mean ± SD. *p < 0.05 versus NTx group; #p < 0.05 versus TTx naïve group. CDK4; cyclin dependent kinase 4, Con; control group, GAPDH; glyceraldehyde 3-phosphate dehydrogenase, NTx; nontransplantation group, PDH; pyruvate dehydrogenase, PHB1; prohibitin 1, PRL-1; phosphatase of regenerating liver-1, SDHA; succinate dehydrogenase, TTx; transplantation group

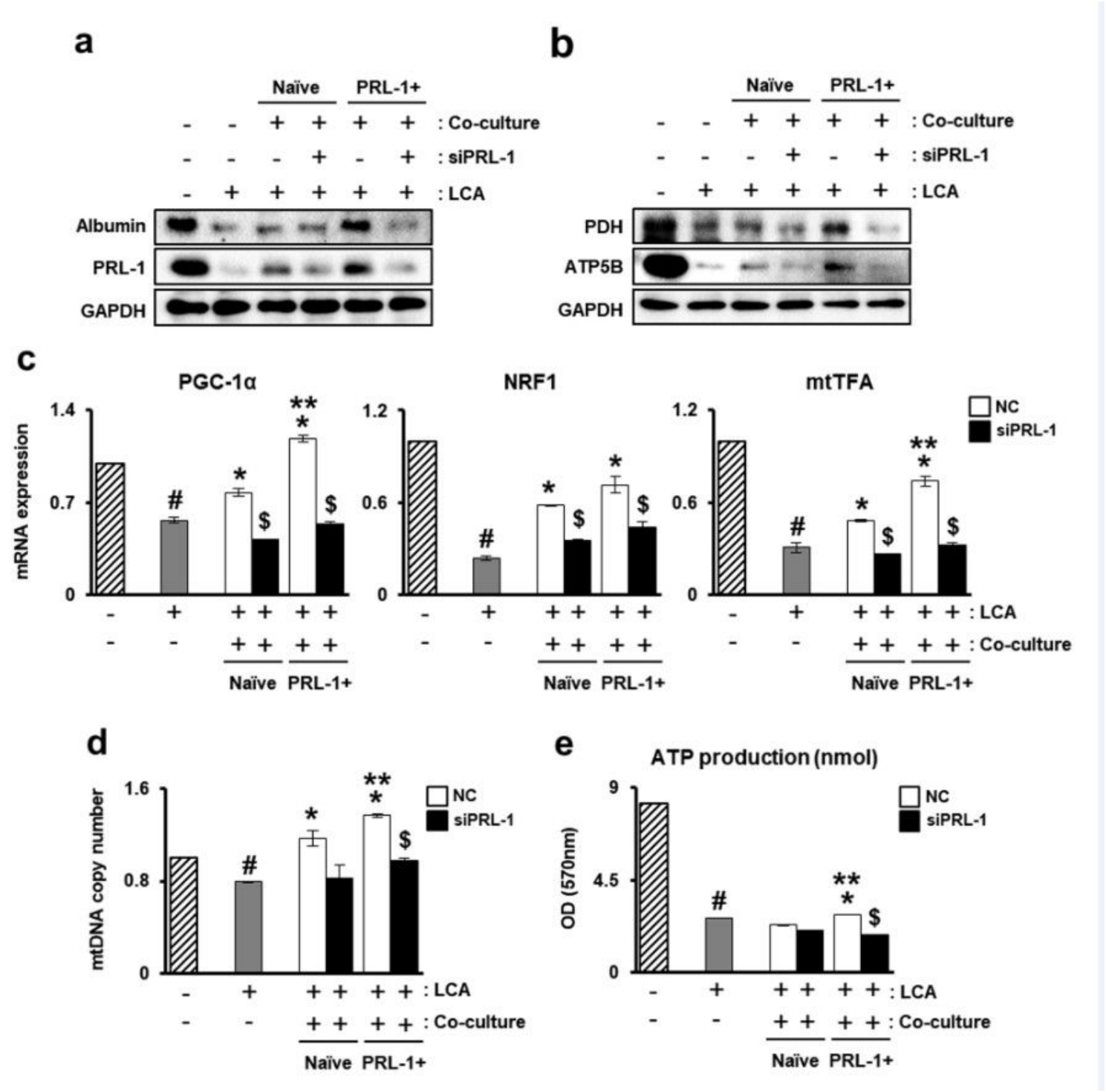

Figure 7

PD-MSCsPRL-1 co-culture activates mitochondrial dynamics of primary hepatocytes. Protein expression of a albumin and PRL-1, b mitochondrial metabolism (PDH and ATP5B) by naïve or PD-MSCsPRL-1 co-culture with or without siRNA-PRL-1 (50nM) for 24 h in primary hepatocyte treated with lithocholic acid (LCA, 100 μM) for 12 h by western blotting. c mRNA expression of mitochondrial dynamics (PGC-1α, NRF1, and mtTFA) by qRT-PCR analysis. d mtDNA copy number in primary hepatocytes by taqman assay. e ATP production analysis in primary hepatocyte lysate (10 μg/μl). Data from each group are presented as mean ± SD. #p < 0.05 versus control (-); *p < 0.05 versus co-culture groups; **p < 0.05 versus naïve; $p < 0.05 versus NC. GAPDH; glyceraldehyde 3-phosphate dehydrogenase, mtTFA; mitochondrial transcription factor A, NC; negative control, NRF1; nuclear respiratory factor 1, PDH; pyruvate dehydrogenase, PGC-1α; peroxisome proliferator-activated receptor-gamma coactivator-1 alpha, PRL-1; phosphatase of regenerating liver-1

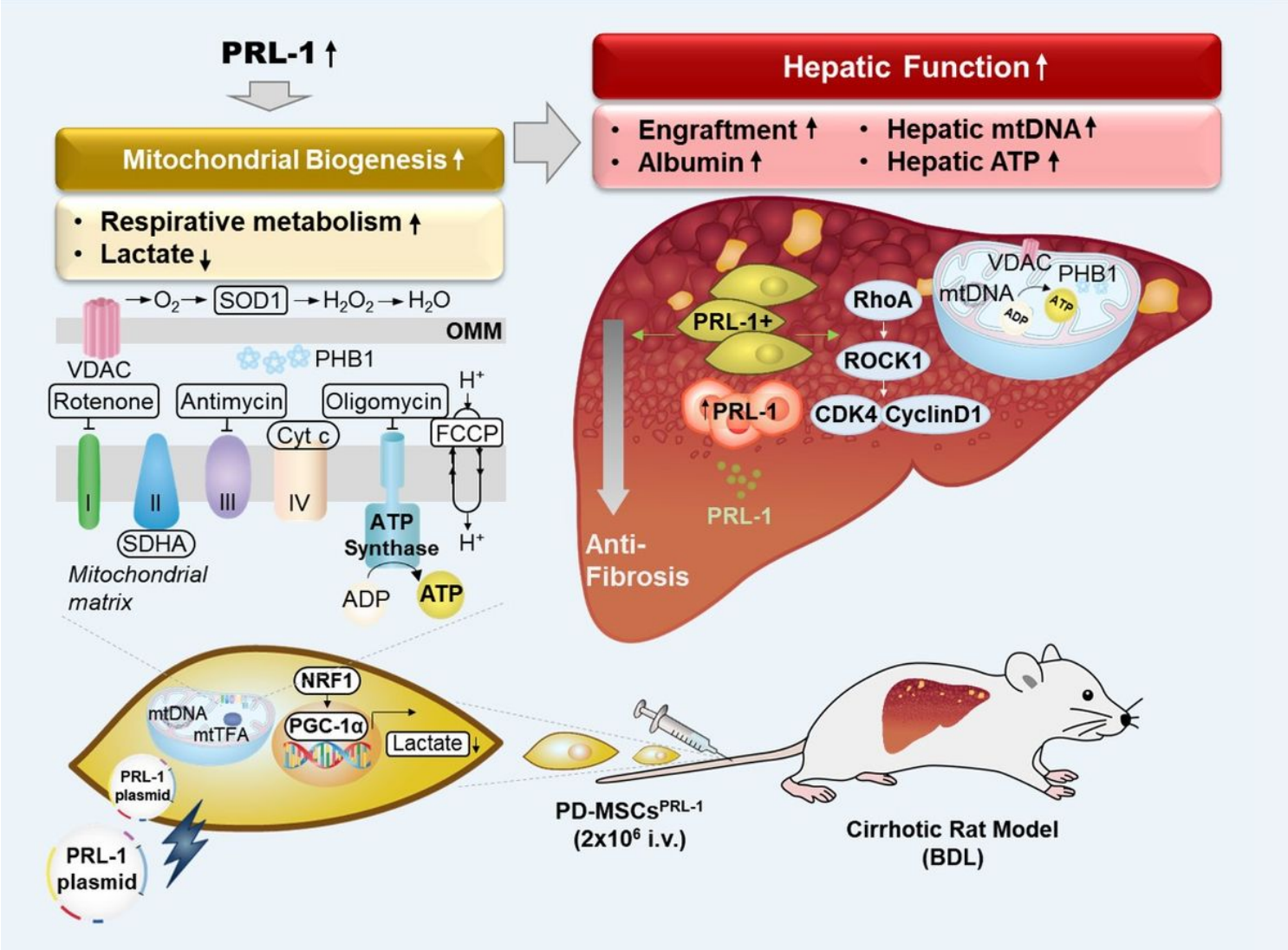

Figure 8

Summarized diagram proposes that PD-MSCsPRL-1 using the non-viral AMAXA system promote mitochondrial respirational states and accelerate liver regeneration by improving hepatic mitochondrial functions. BDL; bile duct ligation, CDK4; cyclin dependent kinase 4, Cyt c; cytochrome c, FCCP; carbonyl

cyanide-p-trifluoromethoxyphenylhydrazone, I.V.; intravenous, mtDNA; mitochondrial DNA, mtTFA; mitochondrial transcription factor A, NRF1; nuclear respiratory factor 1, PD-MSCs; placenta-derived mesenchymal stem cells, PGC1α; peroxisome proliferator-activated receptor-gamma coactivator-1 alpha, PHB1; prohibitin 1, PRL-1; phosphatase of regenerating liver-1, SDHA; succinate dehydrogenase, VDAC; voltage-dependent anion channel